Mapping the photovoltaic potential of the roads including the effect of traffic

Ferri, Carlotta ; Ziar, Hesan; Nguyen, Thien Tin; van Lint, Hans; Zeman, Miro; Isabella, Olindo

DOI
10.1016/j.renene.2021.09.116

Publication date
2022

Document Version
Final published version

Published in
Renewable Energy

Renewable Energy 182 (2022) 427–442

Contents lists available at ScienceDirect

Renewable Energy

journal homepage: www.elsevier.com/locate/renene

Mapping the photovoltaic potential of the roads including the effect of traffic

Carlotta Ferri [a], Hesan Ziar [a, *], Thien Tin Nguyen [b], Hans van Lint [b], Miro Zeman [a], Olindo Isabella [a]

[a] Delft University of Technology, Photovoltaic Materials and Devices Group, Mekelweg 4, 2628 CD Delft, the Netherlands
[b] Delft University of Technology, Transport & Planning Department, Stevinweg 1, 2628 CN Delft, the Netherlands

ARTICLE INFO

Article history:
Received 2 February 2021
Received in revised form
24 September 2021
Accepted 27 September 2021
Available online 2 October 2021

Keywords:
Photovoltaic (PV) technology
Solar road
Traffic shading
Solar potential map
Urban PV

ABSTRACT

After developing the methodology, we applied it to the case of the Netherlands highways. We show that the average irradiation on the Dutch highway network is around 880 kWh/m2/y, 35% less than the potential of an optimally tilted conventional PV system in the south of the Netherlands. Covering the entire 1600 km of the Dutch highways network with solar road modules of poly c-Si, mono c-Si and CIGS would respectively generate 5.2 TWh/y, 6.6 TWh/y, and 3.4 TWh/y of DC electricity. This could be used to fully power the Dutch national public lighting demand. Moreover, to include the effect of traffic on these values, a model was developed to account for the energy potential reduction due to vehicles shading. Using real traffic data from two of the top-four busiest roads in the Netherlands, the A12 and A16, it was found that traffic accounts for an average of 3% reduction of solar road irradiation and DC yield potential. The maximum reduction of 9% was observed in particular locations, such as bridges and nearby ramp roads. The result of such mapping methodology could serve as a useful tool for research advisory, private industry, and governmental projects.

1. Introduction

With cities getting more densely populated and energy demanding, infrastructure integrated photovoltaic (IIPV) technology has gained more interest from researchers, companies, and governmental institutions. What IIPV technology offers in addition to conventional photovoltaic systems is the solution to the land constraint issue [1]. In fact, providing power with a reasonable energy density from photovoltaic technology requires a great amount of land. In Ref. [2], P. Denholm and R. Margolis claim that if the US should be entirely powered by photovoltaic energy, around 180 m^2 per person of land area would be needed, which corresponds to about 0.6% of the total US land area, a dimension comparable with the total area of the Netherlands. This land occupation competes with housing, transportation, and more severely with the agriculture sector. Hence, high deployment of conventional PV systems might raise a future conflict between the agriculture and sustainable energy sectors [3].

All this considered, the idea of integrating photovoltaic technology in already existing built-up surfaces becomes very attractive because no additional space is needed and only a limited infrastructure adjustment is required. Many technological solutions have been already studied and tested, from facades integrated PV to shading objects in the urban environment [4–6]. According to Ref. [7], roads have a great irradiation potential, and the Netherlands Organization for Applied Scientific Research (TNO) claims that the Dutch road network, which accounts for around 135.000 km (including more than 1600 km of highways), converted into solar roads, could harvest enough electricity to cover 10% of the national demand, while one third of the road network could power 9 million cars with clean energy [8].

While there are numerous studies on IIPV potential in urban areas ([4,6,9–11]), the literature and results on solar road potential modelling is currently still very poor [7,12]. Among the most interesting projects there are the study case presented by V. Prasanth et al. [13], where the emergency lane of the Dutch highway A12 is simulated to convert electricity at 9.68% efficiency as solar road, the work of A. Shekhar et al. [1] on the energy performance of the TNO installed solar bike path in Krommenie, Amsterdam, and the research of V. Kumar [14] regarding the temperature model of

* Corresponding author. ;
E-mail address: h.ziar@tudelft.nl (H. Ziar).

https://doi.org/10.1016/j.renene.2021.09.116

TNO solar road technology. The scarcity of material is probably due to the early development stage of the solar road concept. More information related to the technology specifications and development can be found in Refs. [15–20].

The aim of this research project is to provide a methodology to accurately yet quickly estimate and map the annual irradiation and DC yield potential of solar roads. The research does not aim to estimate the technical or economic feasibility of the technology. The methodology considers ambient, urban geometry, and traffic. Electricity conversion, storage and transmission as well as dispatch are not considered in this study. As an example case, we worked on the Dutch highways network, and drafted the irradiation and DC yield potential of solar roads for three different potential PV technologies: monocrystalline silicon (mono c-Si), polycrystalline silicon (poly c-Si) and copper indium gallium selenide (CIGS). Then, for two Dutch highways, a study of the traffic shading has been conducted and insightful information about the evaluation of traffic impact on solar roads yield has been provided. Dutch Highways have been selected for this first research project due to the wide data availability and limited slope. However, the same method could be applied to other roads categories.

The paper is organized as follow. In section 2, the methodology, the irradiation model is introduced, while the data used and the model inputs are further described. A sensitivity analysis of the approach is conducted, based on the model inputs, considering the possibility of limited data quality or computational power. It follows a detailed description of the temperature model applied for the three different PV technologies. Eventually, the traffic shading model is presented. In Section 3, the model results are reported for the case of Dutch highways. An example of the A10 highway is given in order to evaluate the irradiation model and the possible functionalities of the map. The DC yield results are then compared with the output of conventional PV systems. The effect of traffic shading on the study cases of A16 and A12 highways is analyzed and discussed. In section 4, conclusion, the findings of this research are summarized and evaluated.

2. Methodology

When it comes to solar road potential modelling, five main factors need to be considered: (1) the geometry of the skyline profile and, therefore, the shading caused by surrounding objects on the modules, (2) the temperature of the module, (3) the shading caused by vehicles driving on the road surface, (4) the soiling effect, snow and haze and eventually (5) the feasibility of the project itself, considering aspects such as the realization costs, noise limitations, Levelized Cost of Electricity (LCOE), etc. In this research, the first three aspects have been considered, which means that geometry of the skyline, temperature of the module and traffic shading are the only variables used to determine the solar road irradiation and DC potential.

2.1. Skyline profile extraction

In order to account for the shading of the surrounding objects, the model needs to consider the geometry of all around a selected location. Considering the vast amount of land and complexity of urban areas along highways, CAD-based solutions were found to be extremely time demanding. On the other hand, photogrammetry requires very high storage capacity. All this considered, digital surface models (DSMs) are freely available in some countries (e.g. in the Netherlands DSM of the entire country as Actueel Hoogtebestand Nederland (AHN) in an online open-source dataset [21]) and satisfy the minimum requirements to obtain the skyline profiles along the whole national motorways network. DSM represents the natural and built features on Earth's surface.[1] This 3D model is generated with a measurement technique called LiDAR (Light Detecting and Ranging). LiDAR is an optical remote-sensing technique which implements a laser light beam to sample the surface of the Earth, collecting x, y, z measurements. The measurement is performed by a moving vehicle (usually an aircraft, helicopter, drone, or a car) which emits laser pulses that reach the Earth surface, scattered, and reflected back to the vehicle where their time and energy of return is then converted into a height model of the scanned area [22]. In order to eventually extract the skyline profile from the DSM data of the analyzed area, the approach described in Ref. [23] is implemented. The skyline profile consists of a projected 360° image of the objects that surround a location (e.g. PV module installation site) within 1 km radius. Although the DSM represents a good replacement for real-life measurements by providing urban elevation profiles in a digital form, the height data used in this study have a few limitations. (1) the data are likely to be outdated and the resolution is limited. The most detailed images that can be extracted from the online open-source represents the surface of the Netherlands in pixels of 0.5×0.5 m^2. This resolution is the one applied in the model presented here. (2) The DSM has a few intrinsic errors, for instance, it cannot clearly represent vertical surfaces. Since the measurements are taken from above the ground, no information is given about the real shape of the detected objects, which are simply seen as perpendicular walls. Hence, features like trees, bridges or even hanging cables lines and traffic shields are represented as monolithic blocks with vertical walls. In the proximity of these objects, the irradiation potential assessment of solar roads is affected. (3) A LiDAR-based DSM represents the surface area but does not give any additional information about the detected items. To recognize the road network, the Nationaal Wegenbestand (NWB) map which illustrates the entire road network of the Netherlands, is superimposed on the DSM. The coordinates of highway location markers (so-called hecto-points and displaced with a regular distance of 100 m along each lane) are used to represent the roads routes. The use of this map allows to georeference roads in LiDAR data and provides regularly distributed points along roads width and length, which permits to conduct a sensitivity analysis of the model by increasing or reducing their relative distance. How the NWB map is used in the model to extract the skyline profile along the Dutch highways is represented in Fig. 1.

2.2. Irradiation model

Most of the irradiation potential models are based on obtaining the hourly irradiance received at the plane of the array (POA). They consider two groups of parameters, weather-related and geometrical parameters, namely: light intensity and its distribution over the sky, target surface (PV module) tilt and orientation, and the skyline profile of the surrounding [10]. By integrating the hourly irradiance for one year, the annual irradiation is then obtained for a specific location. These values are then further inserted into a thermal and further electrical model to obtain the energy output potential. As it can be noticed, this modelling approach consists of repetitive extensive calculations and, nevertheless, a high amount of meteorological data from the installation site. These are not always available and, therefore, limit the potential of PV system yield modelling. Additionally, the wider the area that it is necessary to consider in the model, the more need for input data [9,24]. Therefore, a different modelling method has been considered for the purpose of this research project.

A different modelling approach was developed in Ref. [11], the so-called simplified skyline-based method, based on the fact that

[1] DSM is different than a terrain model (DTM), which only include bare Earth elevation data.

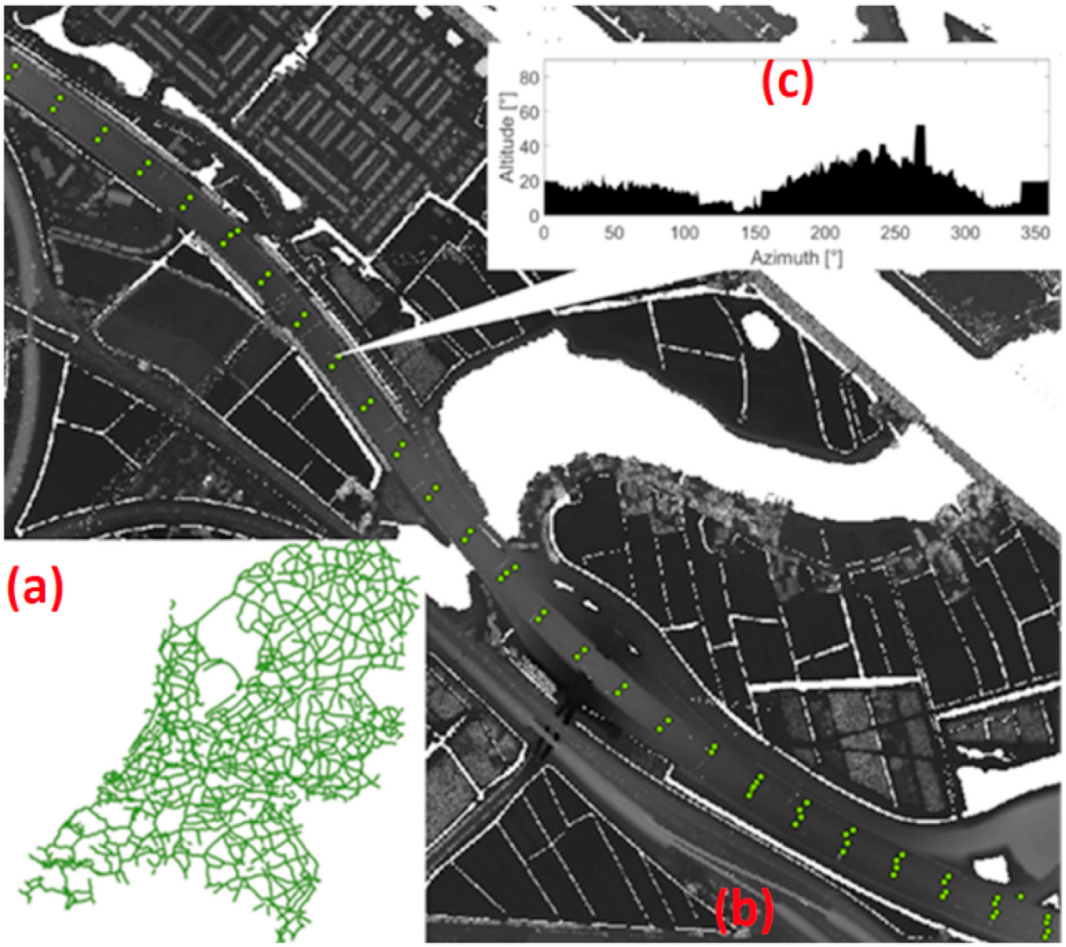

Fig. 1. (a) Dutch road network, **(b)** hecto-points map of the Dutch road network superimposed on a DSM image, and **(c)** an example of projected skyline profile of one selected hecto-point.

weather conditions for a region are similar from one year to another. Hence, it is reasonable to replace weather data with climate data to estimate the annual irradiation on a POA. Therefore, the model can obtain the annual irradiation at a given location using only two geometrical indicators that depend on the skyline profile: sky view factor (SVF) and sun coverage factor (SCF).

The SVF represents the portion of the sky in which the diffuse radiation from the Sun is not blocked by surrounding objects or decreased by the module tilt itself, and reaches the POA [25]. It can be calculated as the fraction of the projected sky dome above the skyline profile. It varies from 0 when the surrounding objects completely cover the sky to 1 when the horizon is completely free.

The SCF is defined as "the ratio between the time that the sun is behind the module or blocked by the skyline per year and the annual sunshine duration at the same location with a clear horizon" [11]. The SCF does not depend on the light intensity, but only on the amount of time that the sun is actually covered by the skyline profile of the surrounding. SCF equals 0 if the horizon is completely free from objects and 1 if the sky view is completely blocked. It can be calculated from Eqs. (1), (1a), and (1b):

$$SCF = \frac{\sum_{year} \chi_{sp}(A_s(t),\ a_s(t))}{\sum_{year} \chi_{fh}(\ a_s(t))} \tag{1}$$

where

$$\chi_{sp}(A_s(t),\ a_s(t)) = \begin{cases} 1 if\ 0 < a_s(t) \le a_{sp}(t) \\ 0 \quad otherwise \end{cases} \tag{1a}$$

$$\chi_{fh}(\ a_s(t)) = \begin{cases} 1\ if\ a_s(t) > 0 \\ 0 \quad otherwise \end{cases} \tag{1b}$$

In Eq. (1), $\boldsymbol{a_s(t)}$ is the altitude of the Sun and $\boldsymbol{a_{sp}(t)}$ is the altitude of the skyline profile.

In [11], it was shown that the SVF and SCF are correlated to the yearly irradiation (Perez irradiance model as reference [26]), respectively, by linear and cubic functions. The correlation between the two indicators and the annual irradiation has been obtained through simulations on both real and synthetic skyline profiles, resulting in five coefficients. The coefficients that describe the curve fitting are valid for a specific module tilt angle and orientation inside a definite climate region. Eventually, the final annual irradiation l can be expressed by Eq. (2) using five empirical irradiation coefficients c_1 to c_5:

$$I_Y = I_Y^{SCF} + I_Y^{SVF} \tag{2}$$

where

$$I_Y^{SCF} = \sum_{i=1}^{i=3} c_i\left(1 - SCF^i\right) \tag{2a}$$

$$I_Y^{SVF} = SVF\left(c_4 + c_5\alpha_{gnd}\right) \tag{2b}$$

where annual sum of the simulated isotropic diffuse and albedo components, referred as I_Y^{SVF} is annual sum of the simulated isotropic diffuse and albedo components (kWh/m^2/year) and I_Y^{SCF} is annual sum of the direct and circumsolar components (kWh/m^2/year). α_{gnd} is the ground albedo.

In [15], it was claimed that the accuracy drop of this model is balanced by the fact that the geometrical factors and empirical irradiation coefficients are easy and fast to obtain. However, in this way, the SCF is not weighted, which means that an object blocking the sun 1 h in the morning and another object blocking the sun 1 h at midday contribute equally in the SCF reduction. This causes a weaker correlation between the model and the hourly irradiation values. In order to correct this weak point of the model, the input for the amount of sunlight received based on the altitude of the sun needs to be corrected. In this paper, we use the concept of *analemma* to apply such correction to the PV yield model of [4]. An analemma describes the position of the Sun, indicated by azimuth and altitude, at a fixed time in day throughout one year. The analemma does not account for a variation of the light intensity with the time, but only for the amount of time that the sun is visible in a specific position of the projected sky dome. Hourly analemmas are the analemmas of each daily hour, projected in a 90° × 360° sky dome matrix. In order to account for this aspect, two correction factors are applied: one based on the so-called optical air mass (AM), and the other one based on the light beam angle of incidence (AoI).

In 1970, experiments conducted in the Mojave Desert of California disclosed a clear correlation between direct irradiance and sun altitude [27]. The irradiance intensity is observed to reduce with increasing zenith angle. This phenomenon is related to an increase of optical air mass and, therefore, the increase of scattering and absorption of light beams in the atmosphere. To account for this effect, the AM is calculated from Eq. (3), formulated in Ref. [28] that considers the Earth's curvature.

$$AM(\theta) = \left(\cos\theta_z + \frac{0.48353\,\theta_z^{0.095846}}{(96.7412 - \theta_z)^{1.754}}\right)^{-1} \tag{3}$$

where θ_Z shows the zenith angle of the Sun position (90°-a_s).

Following this physical concept, the irradiance on a surface consequently increases together with its altitude too. This because the direct sunlight needs to pass through less atmosphere [27]. The relation between direct irradiance component, sun altitude and point elevation (only within the first kilometre of altitude) can be obtained with the empirical relation of Eq. (4), adapted from Ref. [27].

$$I(AM(t), h) = I_0(1 - 1.4h)e^{-0.357AM(t)^{0.678}} \tag{4}$$

with I_0 the solar constant 1361 (W/m^2) [29] and h the altitude of the point of observation (km).

All this considered, a correction factor f_{AM} based on optical air mass is introduced into the model. The factor is defined as the ratio of the actual direct beam for a specific h and AM(t) to the direct beam at AM1, as expressed in Eq. (5). This is because the I(AM1) indicates the maximum direct irradiation that can reach a terrestrial surface after passing the atmosphere. AM1 describes the situation of the Sun positioned at the zenith (α_s = 90°), where the shortest possible path of atmosphere needs to be overcome (around 100 km).

$$f_{AM} = \frac{I(AM(t), h)}{I(AM1)} \tag{5}$$

The AM correction factors varies from 1 when the sun is at the zenith (a_s=90°) and the AM is minimal (AM1) to 0 when the sun is on the horizon (a_s=0°) and AM is maximal (AM26).

To account for a correction factor based on the angle of incidence of the light beam, the Lambert cosine law is applied. It states that the direct irradiance on the POA is directly proportional to the cosine of the AoI. From this effect it can be said that the solid angle, from which the sunbeams can reach the module surface, becomes smaller with increasing AoI. To compensate this effect, the correction factor of f_{AoI} is obtained from (Eq. (6)):

$$f_{AoI} = \cos\theta_M\cos\theta_Z + \sin\theta_M\sin\theta_Z\cos(A_S - A_M) \tag{6}$$

where θ_M and A_M are the tilt and orientation of the module. A_S is the Sun azimuth. For modules with a tilt angle equal to zero (θ_M = 0), which corresponds to the approximation considered in this report for solar roads,[2] the correction factor shown in Eq. (6) is simplified to the cosine of the zenith angle. This approximation is suitable for the case of the Netherlands where the landscape does not show high variation of altitude per unit of area. In fact, by following changes in altitude, roads can have varying slopes. Being solar road modules integrated in the road surface, these changing tilts should be integrated in the model if applied to other landscapes. In case the model needs to be implemented on roads whose slopes are not negligible, in Eq. (6), θ_M should corresponds to the slope of the road.

Fig. 2 compares the hourly analemmas of the model developed in Ref. [15] (on the left) and the one corrected with the AM and AoI correction factors in this paper (on the right). It can be noticed how the product of the two correction factors strongly reduces the amount of irradiation received by a solar road. In particular, the irradiation coming from the Sun altitude up to 10° is completely invisible for a PV module placed on a horizontal surface while it is strongly reduced between the Sun altitude angles of 15° and 20°.

2.3. DC yield model

Once the annual irradiation potential of a PV system is known, its operating efficiency needs to be calculated to obtain the annual DC yield output. The empirical correlation proposed for the irradiation model can be applied for the DC yield model as well. This means that the annual DC yield output that can be expressed in Eq. (7), using five other empirical DC yield coefficients of d_1 to d_5 [15].

$$E_Y = E_Y^{SCF} + E_Y^{SVF} \tag{7}$$

where

$$E_Y^{SCF} = \sum_{i=1}^{i=3} d_i\left(1 - SCF^i\right) \tag{7a}$$

$$E_Y^{SVF} = SVF\left(d_4 + d_5\alpha_{gnd}\right) \tag{7b}$$

The DC yield coefficients d_1 to d_5 are valid for a specific PV module type and tilt. In the model presented in this paper the assumption is made that the module type and tilt are fixed along the road, making the approach described in section 2.3 suitable for

[2] Normally roads have a camber up to 3% (1.7°) for drainage purposes. This angle tilt is neglected in the model.

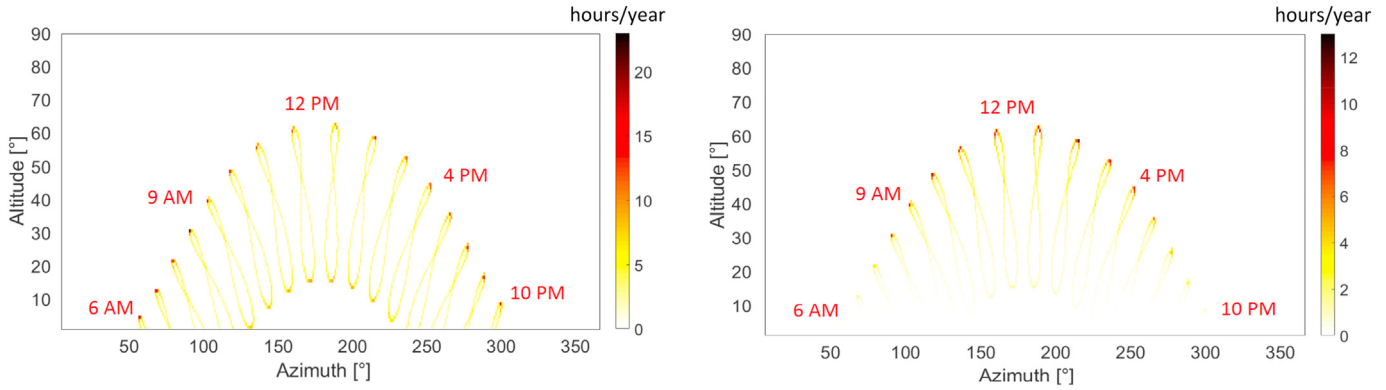

Fig. 2. Examples of hours per year in which the Sun is seen by a solar road module projected in the sky dome in each hourly analemma: (left) before correction, (right) after implementation of the AM and AoI correction factors [hours/year].

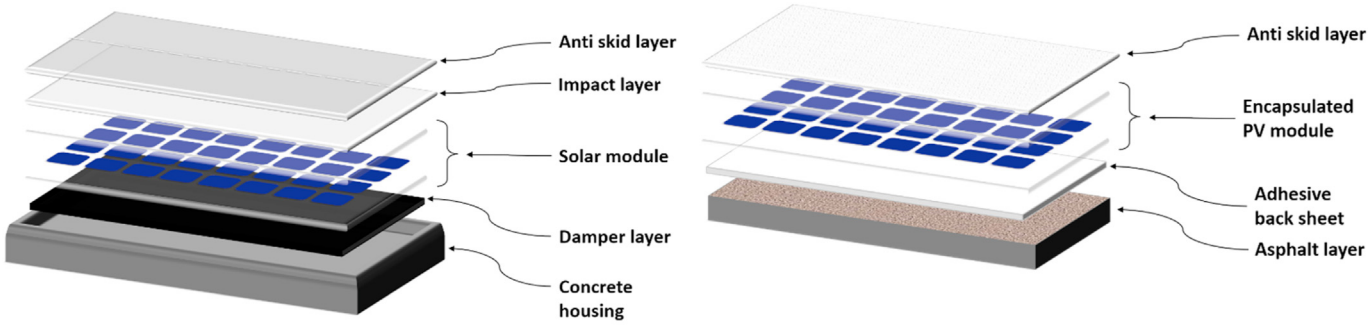

(a) **(b)**

Fig. 3. Sketches (a) of a TNO SolaRoad section and (b) of the solar road module concept applied in this project, inspired by the Wattway solar road technology.

DC yield analysis of long distances on roads and highways. However, as already mentioned, these assumptions are reasonable only if applied to an area with limited high differences, like the Netherlands, where the model is applied.

In order to obtain the DC yield coefficients for solar road technologies, a modification of the temperature model is necessary. In the case of a solar road, the thermal behavior of the module needs to be considered differently than conventional modules. The temperature of the module is influenced by the irradiance intensity on the array top surface, its radiative emission and the conductive heat transfer between the layers. Since the cells are placed between an anti-skid layer and the asphalt (see Fig. 3), the cooling effect of wind and surrounding air on the rear side does not take place. On the other hand, the underneath soil absorbs the heat, playing the role of heat sink [1]. Any heat exchange caused by traffic on the solar road is neglected in this study.

In [14], a thermal model was proposed to estimate the temperature of the solar cells in the SolarRoad concept developed by TNO and tested in Krommenie, the Netherlands 2014. The model was built upon the fluid dynamic model described in Ref. [30] with the integration of conductive heat exchange between the layers. A one-dimensional heat transfer is considered since all the materials have low thermal conductivity and because the dimensions of width and length (in the order of 10^1 m) are much bigger than thickness (in the order of 10^{-3} m). Applying the temperature model described in Ref. [26], the five DC yield coefficients for SolarRoad technology are obtained (see Table A2 in the Appendix).

2.4. Traffic shading model

To consider the effect of traffic shading in the model, traffic data of vehicles flow q (veh/h) and speed u)km/h) should be considered. These data are collected with vehicle loop detectors.[3] Vehicles' flow and speed are represented in the examples of a section of the highway A16 in Fig. 4.

For each speed and flow value, the coordinates of the measurement points were used to generate a geographical distribution of the data. The route is then interpolated and described using 200 m distanced points along the highways.

The time that the vehicle needs to completely surpass a very small part of the highway (e.g. equal to the size of a PV module) with the length of l can be defined as in Eq. (8).

$$\Delta t = \frac{d + l}{u(t)} \tag{8}$$

where d is the length of the vehicle, here assumed to be 5 m (0.005 km), and $u(t)$ is the travelling speed of the vehicle at the moment t. The cumulative time in which the point is shaded by passing vehicles (T_{tr}) can be calculated as in Eq. (9).

[3] The most common detectors are based on inductive loop: a wire coiled in a circle below the road surface detects the variation of the electric field and can detect when a vehicle passes over the loop and at which speed.

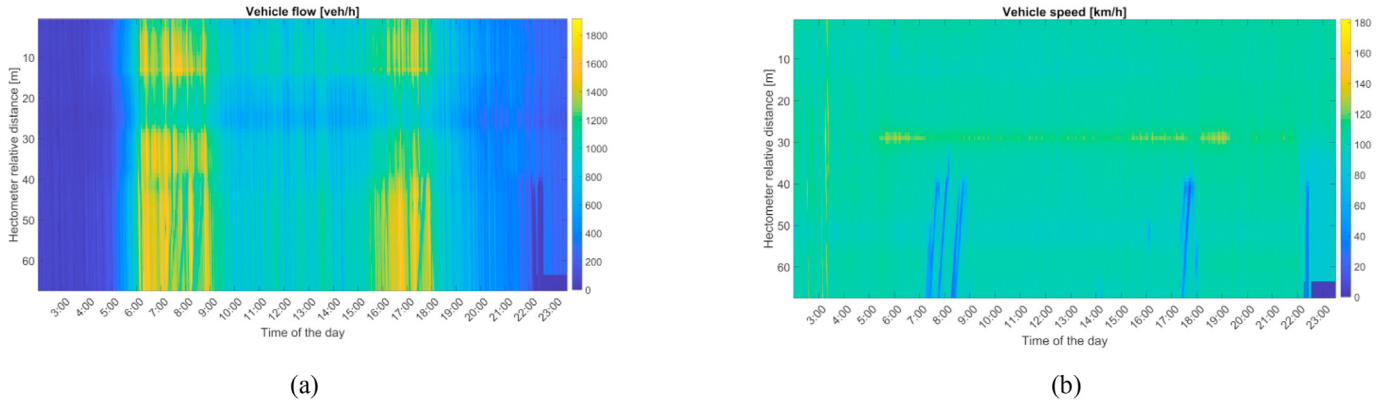

(a) (b)

Fig. 4. Vehicles (a) flow and (b) speed obtained from the highway A16 (15–30 km) left lane on the June 4, 2018. Drawing a horizontal line perpendicular to the y axis, the variation of vehicles' speed or flow throughout the day in a specific point of the road can be obtained. Similarly, following a vertical line perpendicular to the x axes discloses the different vehicle speeds or flows that are encountered in a specific moment of the day along different sections of the road.

$$T_{tr} = q(t)\Delta t \tag{9}$$

where $q(t)$ is the vehicles flow (veh/h) at the moment t. T_{tr} is a vector that indicates the minutes in each hour (min/h) of the day during which the point is shaded by passing vehicles. The coverage time T_{tr} can be seen as a reduction of the time in which the sun is shining on the solar road point.

However, the impact of the shading caused by a car passing above the road surface varies with time. In fact, a car shading a point of the road surface at noon will have a stronger impact on the reduction of the total daily irradiation if compared with a car shading for the same time the same point in the evening. For this reason, T_{tr} needs to be weighted depending on the moment of the day and, then, deducted from the hourly analemmas in order to estimate the effective irradiation that reaches the road surface. Knowing the T_{tr} at each hour of the year, it is possible to correlate it to a specific position of the Sun in the sky dome. Therefore, the T_{tr} can be represented in the same way as hourly analemmas which allow adding weight to this factor. Fig. 5 depicts an example of hourly traffic shading analemmas for a point on the A16. The plot shows the time (in minutes) in which the solar road point cannot see the Sun in its time-specific position in the sky dome due to traffic shading. This is represented for an entire year with an analemma for each hour of the day.

In order to correct the total irradiation of one point with traffic shading, SCF and SVF need to be adjusted. The SCF of Eq. (1) can therefore be redefined as traffic coverage factor (TCF) in Eq. (10). The traffic coverage factor corresponds to the: (i) the sum of the hours in which the sun is behind the elevated skyline (SCF), added to (ii) the time in which the sun is above the skyline profile but the point is shaded by passing vehicles, divided by the total amount of hours in which the sun is above the horizon:

$$TCF = \frac{\sum_{year} \chi_{sp+tr}(A_s(t),\ a_s(t))}{\sum_{year} \chi_{fh}(\ a_s(t))} \tag{10}$$

where

$$\chi_{sp+tr}(A_s(t),\ a_s(t)) = \begin{cases} 1 if\ 0 < a_s(t) \le a_{sp}(t) \\ T_{tr}(A_s(t),\ a_s(t)) \quad otherwise \end{cases} \tag{10a}$$

$$\chi_{fh}(\ a_s(t)) = \begin{cases} 1\ if\ a_s(t) > 0 \\ 0 \quad otherwise \end{cases} \tag{10b}$$

The SVF can be corrected to a traffic view factor (TVF) applying a shading factor due to traffic f_{tr}, as in Eqs. (11) and (12). TVF can be generated as the ratio between the corrected analemmas that consider the traffic shading (the hourly traffic shading analemmas are subtracted by the hourly Sun analemmas), and the ones that do not. The traffic shading coefficient varies from 0 in case the traffic completely blocks the sunlight on the road surface for the entire year, to 1 in case the point never occurs to be shaded by vehicles throughout the year.

$$f_{tr} = \frac{sunMat - trMat}{sunMat} \tag{11}$$

$$TVF = f_{tr}\ SVF \tag{12}$$

where *sunMat* refers to the matrix representing the hourly Sun analemmas, including the AM and AoI correction factors and the skyline profile, while *trMat* describes matrix representing the hourly traffic shading analemmas. Using the TVF and the TCF, respectively instead of SCF and SVF in Eqs. (2) and (7), allows to estimate the irradiation and DC yield potential of a solar road, considering real traffic data.

3. Results

3.1. Improvement of the irradiation model accuracy

The solar radiation received on Earth depends on the weather and air mass that the sunlight passes through. It is, therefore, mainly dependent on locations latitude [27]. Hence, the impact of the AM based correction factor on the accuracy of the irradiation model is studied for higher and lower latitudes, in order to explore the sensitivity of the corrected model. In addition to the two locations selected in Ref. [11], Delft (The Netherlands, Lat 52.0116°, Long 4.3571°) and Antofagasta (Chile, Lat −23.6483°, Long −70.3984°), two other cities are considered, Reykjavik (Iceland, Lat 64.142391°, Long −21.933422°) and Bata (Equatorial Guinea, Lat 1.856503°, Long 9.766125°) which are situated respectively at higher and lower latitudes. For each of these cities, a comparison is conducted between the coefficients obtained with the original model (where no AM correction factor was applied) and with the improved version. The results of the analysis for Delft and Antofagasta are shown in Fig. 6.

It can be observed that applying a correction factor based on the optical air mass improves the coefficients for low tilt angles. In particular, for higher latitudes (Delft and Reykjavik), the accuracy of

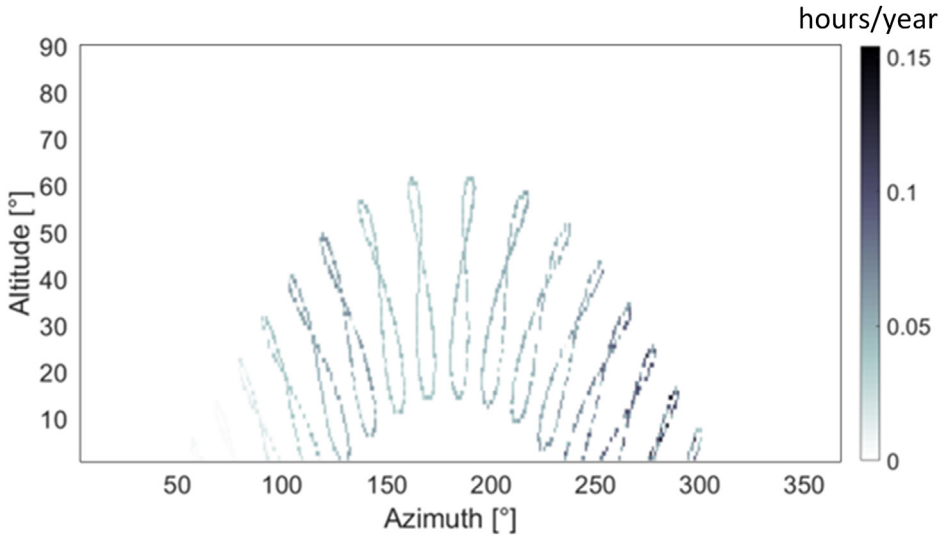

Fig. 5. Hourly traffic shading analemmas of a point along the A16 [hours/year]. It represents how many hours in a year the Sun is not visible at each position of each projected sky dome to the solar road point due to traffic. Each analemma represents this for a specific hour of the day throughout the year. A higher traffic shading in the morning hours can be recognized.

the model stabilizes on a constant value around 0.99, whereas in the previous version of the model it was linearly decreasing with the tilt angle. In the case of lower latitudes (Antofagasta and Bata), the improvement of the model is less significant. This is because not considering the AM correction factor overestimates the radiation at high zenith angles (when the sun is low on the horizon) in the original model. The conditions of high zenith angles for Sun altitudes are more often in the case of Delft and Reykjavik since they are located at higher latitudes. In fact, the variation of the Sun altitude throughout the year is directly proportional to the latitude of the location where it is observed. Therefore, moving from Reykjavik to Delft, to Antofagasta and eventually to Bata the overestimation of direct sunlight at high zenith angles decreases its impact on the irradiation estimation.

The same can be said for low module tilt angles. For a module placed horizontally on the ground (0° tilt), as assumed in this model applied to the Netherlands, the share on total POA irradiation is higher for the diffuse than for the direct component, due to the orientation. An overestimation of the Direct Normal Irradiance (DNI) reduces the accuracy of the total irradiation estimation for these modules.

To conclude, it can be stated, that introducing the AM correction factor improves the correlation of the model with the DNI. The influence of DNI on low tilt angles at higher latitudes is lower than at lower latitudes. By reducing the influence of the DNI component with increasing latitude due to air mass, the model is now more accurate. The improvement still has a limited magnitude due to the fact that the locations that most benefit from the improved correlation with DNI (higher latitudes) are mostly the ones where the share of DNI component is less significant.

In fact, the major improvement to the model accuracy is provided by the AoI correction factor. As shown in the comparison in Fig. 7, after applying the AoI correction factor for 0° tilted modules, 94% of the results fell within 5% of relative deviation from the simulated values. In comparison, the previous version of the model was giving a 5% range of relative deviation for only 66% of the values.

3.2. Sensitivity analysis

To analyse the impact of skyline profile resolution on the estimated irradiation, a sensitivity analysis based on the increase of the azimuth step angle is conducted. The aim of this analysis is to evaluate the gain in computational time against the loss of accuracy in the irradiation potential estimation of a point and eventually suggest the optimal trade-off between the two aspects. The analysis is applied to a sample of 496 points taken from a section of the A16 highway. Instead of every

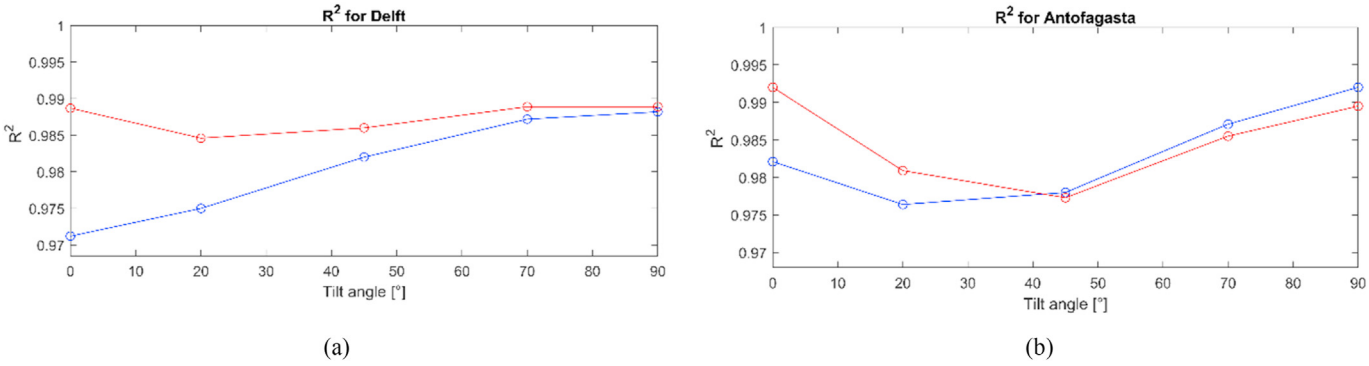

Fig. 6. Improvement of accuracy in the model with implementation of the AM correction factor: the blue line shows the accuracy of the original model expressed with R^2 versus module tilt angle. The red line represents the accuracy of the improved model after the implementation of the AM correction factor. Examples for (a) Delft (the Netherlands) and (b) Antofagasta (Chile).

1°, the presence of obstacles is detected for every 2°, 5°, 10°, and 20°. The obtained profiles are eventually interpolated to generate the skyline projections (see Fig. 8). The results are then evaluated in order to find the optimal azimuth step angle.

Fig. 9 shows the results of the sensitivity analysis. It can be observed that by reducing the step angle, the maximum number of calculations necessary when extracting the skyline profile decreases exponentially. However, this increases the percentage of deviation of the results from the reference values obtained with 1° azimuth step angle in an almost linear correlation. The optimal point is found at 5° azimuth step angle. This would lead to a reduction of 80% of the number of calculations and a deviation below 2% in the obtained irradiation values. Still, an azimuth step angle of 1° is kept in the model.

An additional sensitivity analysis was conducted on the points density along the road. The objective of this sensitivity analysis was to investigate how the density of points distribution along the road impacts the results. The analysis consists a systematic increase of the point-to-point distance (hereafter referred as relative points distance) from 1 to 10, 20, 50, 100, 200, 500 and 1000 m on the road length for 7.4 km along the A16. The skyline profile extraction and the irradiation model are then applied to each of the obtained points. Fig. 10 shows the absolute deviation from the reference irradiation that can be observed in the points sample by increasing the points relative distance. It is still possible to represent the average and peak irradiation along the road with a deviation lower than 2% from the reference case. However, after 100 m of relative distance, values start to vary more largely and the deviation grows up. This is due to the fact that the skyline profile does not follow any pattern and it is rather random. Therefore, when the points are more densely distributed, more details about specific points will be captured. If the points are less densely distributed, it is more probable to miss peaks

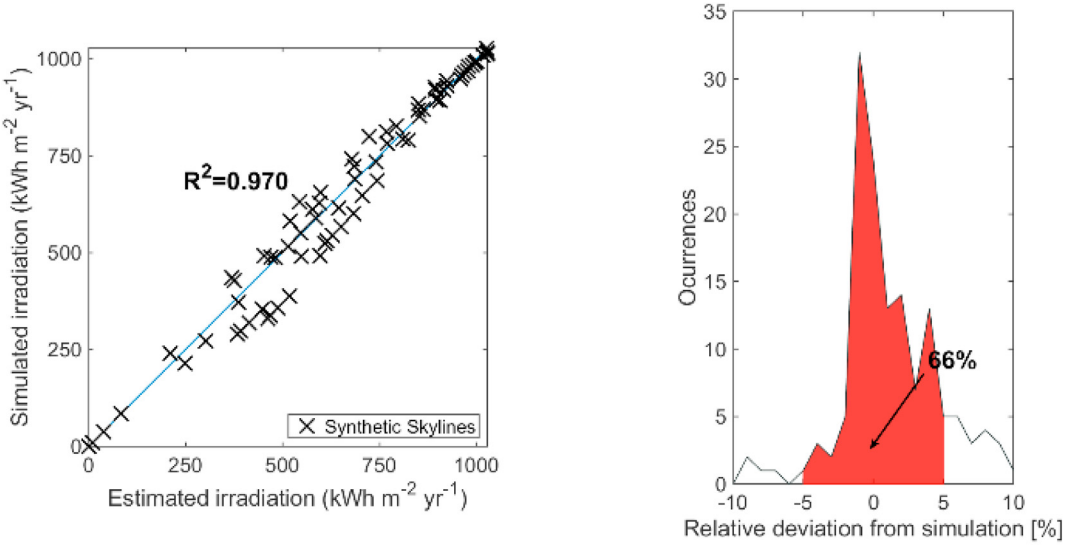

(a)

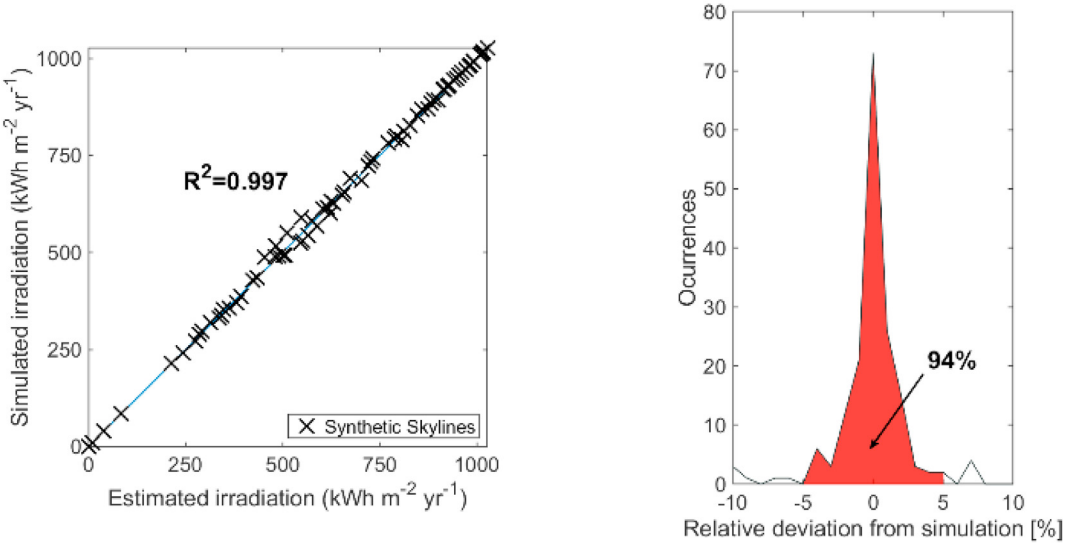

(b)

Fig. 7. Comparison of the relative standard deviation and coefficient of deviation for the original (a) and improved (b) version of the irradiation model for 0° tilted modules (Images generated from the original model described in Ref. [15]).

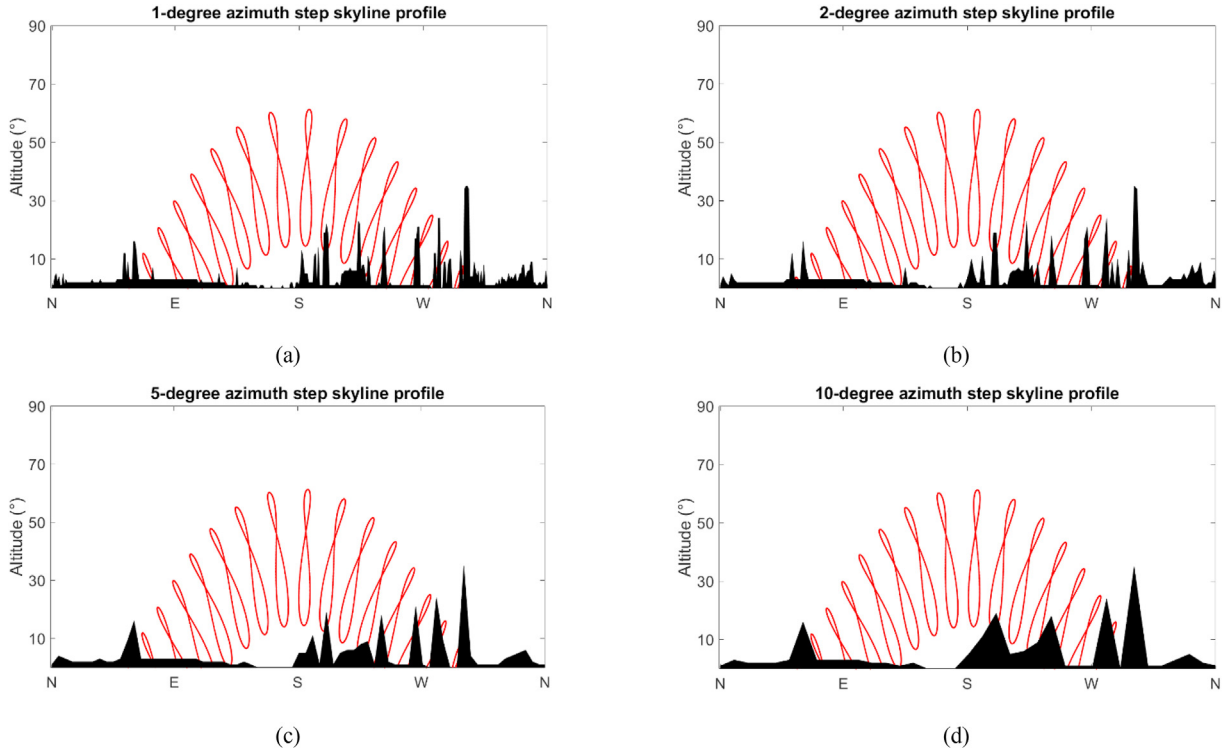

Fig. 8. Examples of how the skyline profile changes by tuning the azimuth step angle from the reference case (a) 1° to (b) 2°, (c) 5° and (d) 10°.

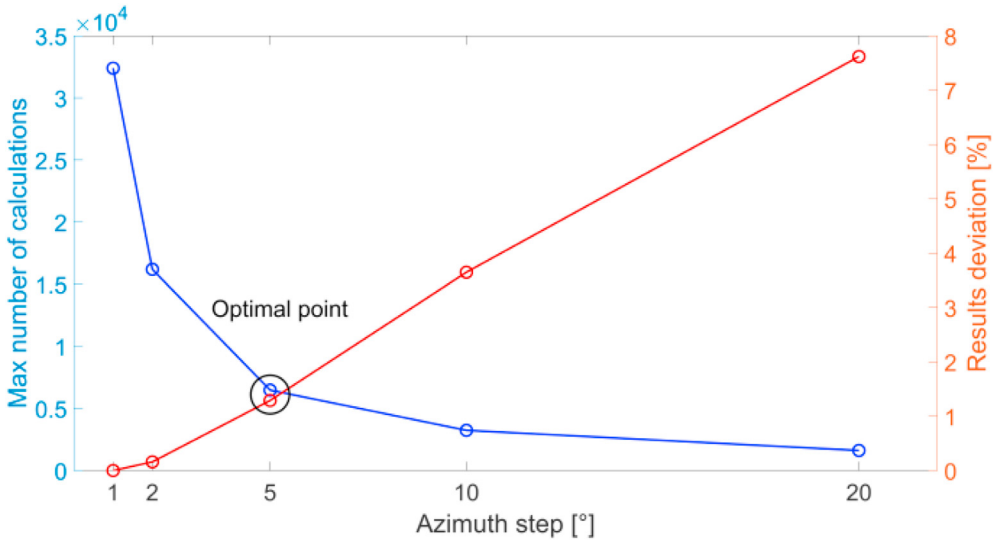

Fig. 9. Maximum number of calculations and deviation of the irradiation results by increasing the azimuth step angle from the reference model (1 m relative points distance).

of maximum and minimum irradiation. As it can be seen in Fig. 10, deviation from average experiences a step at 10 and 100 m. To be at a reasonable error level and decrease the computation time as much as possible, point step of 100m was chosen. The relative distance of 100 m at which the data are provided in the hecto-points map shows a 0.4% deviation from the reference average and 1.6% deviation from the maximum reference values.

3.3. Irradiation potential

After having applied the improvements described in Section 2, the five irradiation coefficients for solar roads in the Netherlands are generated. To derive more accurate irradiation coefficients, the Netherlands was divided into two climatological regions: the South-West and the North-East. This is due to the fact that the country shows a variation of irradiation potential moving from South-West to North-East [31]. The climate data of two cities within these regions, Delft (52.0116, 4.3571) and Leeuwarden (53.2012, 5.7999) respectively, are used to generate the irradiation coefficients for the two areas. The obtained coefficients can be found in Table A1 in the Appendix.

For each of the hecto-points used to describe the Dutch

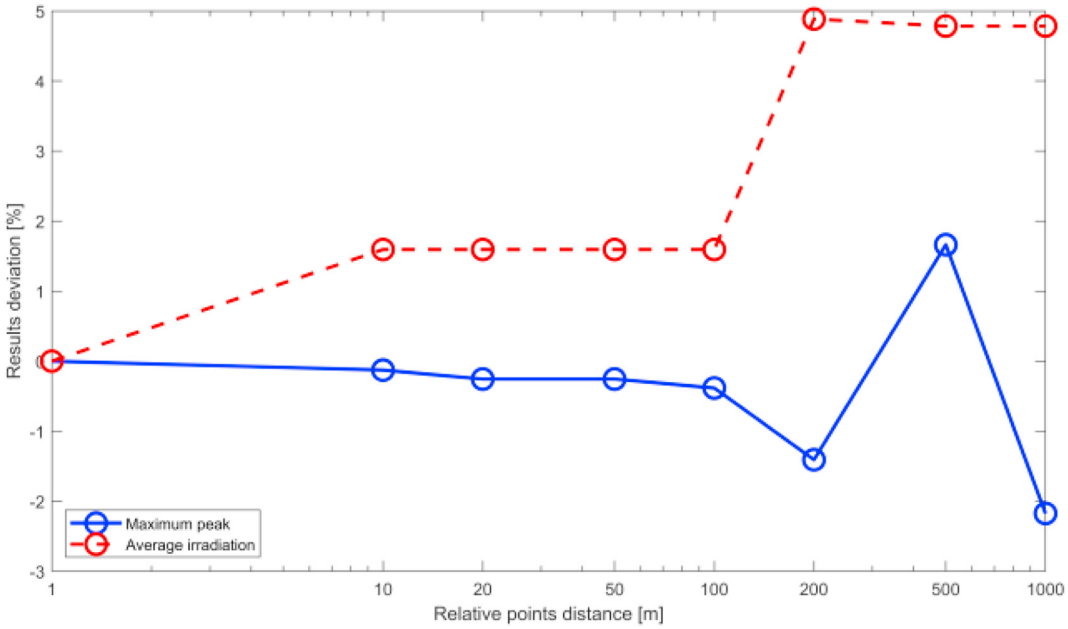

Fig. 10. Irradiation model results deviation by increasing relative points distance from the reference model (1 m relative points distance).

highways network, the SVF and SCF are obtained from the projected skyline profile and the irradiation model is applied to the Dutch highways, using different irradiation coefficients for roads situated in the South-West and in the North-East part of the country. Fig. B1 in the Appendix shows the graphic results of the model, where the simulations conducted for every 100 m of length and 15 m of width while the rest of the points are interpolated.

Overall, Dutch highways show an average irradiation potential of 882 kWh/m^2/y and a maximum peak on A73 of 1026 kWh/m^2/y. The top three most irradiated highways are A31, A5 and A200, as reported in Table 1. The map also brings the possibility to investigate the potential for solar road installation with higher spatial resolution. Fig. 11 depicts the irradiation potential of highway A10 around Amsterdam. It is a very useful example to evaluate locations for a solar road installation project. An area where the construction of a solar road is not advised would be the section indicated with the box no. 1. As it can be observed in the picture, trees planted along the road at the interchange and that an intersecting road decrease the irradiation potential in the area to an average of 670 kWh/m^2/y. On the other hand, the section indicated with the box no. 2 represents an appealing location for solar road installation with an average irradiation potential of 940 kWh/m^2/y.

Over the Dutch highway network, there are several locations in which the irradiation potential has been observed to drop. From further and broader analysis, it has been recognized that reduction of irradiation potential is mainly caused by the following four factors: (i) underpasses at interchanges and bridges, (ii) tree-lined avenues, (iii) urban environment, and (iv) distorted data (traffic shields, transmission cables, etc.).

Table 1
Irradiation and DC yield of the three most irradiated highways.

Average (kWh/m^2/y)	A31	A5	A200
Irradiation	1002	999	983
poly c-Si (DC yield)	157	157	154
mono c-Si (DC yield)	196	196	193
CIGS (DC yield)	105	105	101

3.4. DC yield potential

The DC yield model is applied to the Dutch highways, using the approach described in Section 2.3 (the DC yield coefficients shown in Table A2). Again, it is chosen to divide the Netherlands into the same two regions used for the irradiation model, the South-West and the North-East. Similar to the irradiation map, Fig. B2 in the Appendix shows the interpolated results of the DC yield model assuming that the highways are covered with poly c-Si technology.

For mono c-Si, Dutch highways show an average output of 173 kWh/m^2/y and a maximum peak of almost 201 kWh/m^2/y in several sites. If poly c-Si is assumed, then the average output decreases to almost 139 kWh/m^2/y, with peaks of 160 kWh/m^2/y in the best locations. With CIGS, the annual DC yield is further reduced to an average of 90 kWh/m^2/y and a maximum value of 105 kWh/m^2/y.

If the total surface of the Dutch highway network was covered by solar road modules, 5.2 TWh/y, 6.6 TWh/y, and 3.4 TWh/y of electricity could be generated in the case of poly c-Si, mono c-Si and CIGS module technologies, respectively. The Netherlands CBS (Centraal Bureau voor de Statistiek) reports a national electricity consumption of 120 TWh in the year 2018 [32]. From 3 to 5% of the national consumption could, therefore, be obtained from solar road installations in the Netherlands. If it is considered that public lighting accounts for around 1.2% of national electricity consumption [33,34], solar highways alone would then be able to entirely power Dutch street lighting, without considering conversion, storage (if applicable) and distribution losses.

3.5. Traffic shading effect

The traffic shading model has been applied for two case studies of highways A16 and A12 in order to observe the effect of traffic on their energy output. According CBS, A16 and A12 are within the top four busiest roads in the Netherlands [35]. The A16 (58 km) connects the city of Rotterdam with the Belgian border, while the A12 (137 km) goes from the city of The Hague to the German border.

The data are provided for one point each 200 m, for both left and right lanes. The data of vehicles flow and speed are converted into the

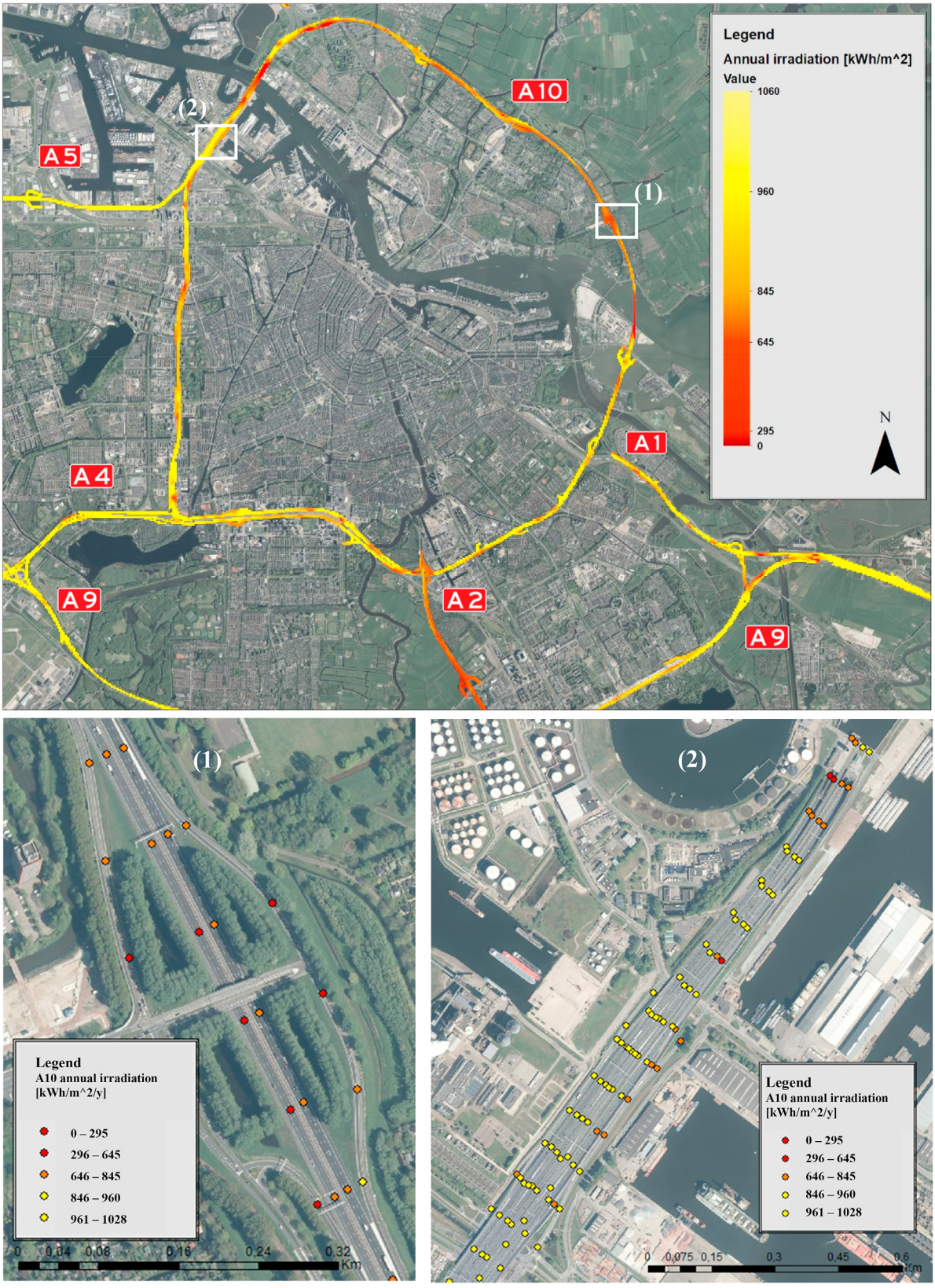

Fig. 11. Irradiation potential map of the Amsterdam ring road A10 with main injecting highways. The map helps to recognize the location where building solar roads is not advised, and also to individuate optimal installation sites.

amount of time in which a solar road point is completely shaded by a vehicle at each hour of the day, called traffic coverage time. Figs. B3 and B4 in the Appendix indicate the interpolation of the cumulative traffic coverage hours obtained for every 200 m along the A16 and A12, respectively. The areas indicated in red are the road sections most affected by traffic shading and are, therefore, the ones that show the highest reduction of the annual irradiation potential.

Overall, the annual average coverage time on the A12 counts for around 240 h, varying from a minimum of 120 to a maximum of 450 h/y. This means that, on average, a point on the A12 is completely shaded due to traffic for a cumulative amount of 240 h/y. For A16 the numbers are slightly lower, with an average coverage time of 230 h/y, varying from a minimum of 58 to a maximum of 416 h/y.

On average, the annual irradiation and DC yield reduction caused by traffic has been found to be around 3% among all the analyzed highways. This shows that traffic shading does not drastically affect solar roads potential. However, this percentage points losses which are comparable with inverter losses and needs, therefore, to be taken into consideration [36,37].

Within A12 and A16, there are specific locations where the reduction rises over 5% for the irradiation and to almost 9% for the DC yield. On the A12, these points are located in proximity to two very large interchanges called in Dutch Knooppunt Lunetten and Knooppunt Velperbroek, located in the province of Utrecht and in the region of Arnhem, respectively. It can be stated that interchanges usually attract high vehicles flows. Additionally, in the proximity of ramps, vehicles speed tends to reduce and the number of lanes decreases as well, generating downstream congestion. A similar effect can be observed at the exit of the highway, where the vehicles need to slow down. These phenomena have been observed to cause a reduction of received irradiation up to 50 kWh in a year. In the case of A16, there are fewer points where the traffic coverage time surpasses the 350 h/y.

3.6. Computational time

As simulation time heavily depends on the complexity of the geometry around a point (generating the skyline profile from the LiDAR data), a set of 537 randomly selected points over the A16 highway was used to calculated the simulation time. On average, each point takes 3.58 s to be simulated excluding the effect of traffic while adding traffic rounds the simulation time up to 4 s per point. A16 is 58 km (2960 points) and, thus, the simulation approach scans over the PV potential over A16 with the speed of 17.6 km/h (3.3 h). The same process was repeated for A12 with 691 randomly selected points, which resulted in 4.38 s simulation time per point. For A12 (137 km with 3255 total points), the simulation speed is 34.6 km/h (3.96 h). It shows that no matter the complexity of the horizon around the road, it takes rather a fix amount time to simulate each point. The key factors affecting the simulation speed over roads are: (1) angular resolution of horizon scanning, and (2) density of the points on the road, which depends on the number of the lanes, connections, roundabouts, etc. Since the research was conducted to prove the concept of large-scale road potential for PV installation, further optimization of the code to reduce the simulation time was not considered.

4. Conclusion

The open-source map of the hecto-points along the main Dutch roads is used to identify the locations of the points along the road where the model is applied. The points have a relative distance of 100 m in the length of the road and of 15 m in the width. From a DSM of the Netherlands, the skyline profiles of these points were extracted. To obtain the irradiation and DC yield potential of solar highways, the simplified skyline-based method was adopted and further evolved. Two main corrections were applied to the model based on the concept of analemma: air mass (AM) and angle of incidence (AoI) corrections. These modifications resulted in a significant increase of the model accuracy, with 94% of the model results deviate only 5% from the values obtained with the reference model (Perez irradiance model), instead of the previous 66%. Assuming the SolarRoad concept developed by TNO, a thermal model based on [13] was also implemented. Eventually, maps of the irradiation and DC yield potentials of solar highways for the whole Netherlands were generated.

Additionally, a traffic shading model, based on real traffic data, is developed to estimate the irradiation that is shaded by passing vehicles on a solar road. To account for traffic shading in addition to the skyline profile, the traffic coverage time is used to correct the SCF and SVF into traffic coverage factor (TCF) and traffic view factor (TVF), respectively. The model is applied to the highways A12 and A16, chosen among the four busiest roads in the Netherlands. The paper showed that traffic has a limited effect on PV yield output (3%) and up to 5% of the Dutch electricity consumption could be obtained from solar road installations. It shows the significant potential of road surfaces as a mean to reduce the CO2 emission.

The solar road map discloses the potential of solar road technology and could serve for advisory and counselling public and private Sectors. The map is a useful tool for recognizing the optimal sites in terms of irradiation, traffic shading, PV technology, and, cost. In order to allow this model to be more widely used in countries were roads and highways show higher slopes and tilts, the model should be improved to take into account the actual tilt of the solar road modules on the road surface.

CRediT authorship contribution statement

Carlotta Ferri: Conceptualization, Methodology, Software, Formal analysis, Investigation, Visualization, Writing – original draft, Writing – review & editing. **Hesan Ziar:** Methodology, Software, Formal analysis, Investigation, Visualization, Resources, Writing – review & editing, (Daily), Supervision. **Thien Tin Nguyen:** Data curation. **Hans van Lint:** Data curation, Writing – review & editing. **Miro Zeman:** Resources. **Olindo Isabella:** Conceptualization, Resources, Supervision.

Declaration of competing interest

The authors declare that they have no known competing financial interests or personal relationships that could have appeared to influence the work reported in this paper.

Appendix

A. Irradiation and DC yield coefficients

Table A1
Irradiation coefficients for 0° tilted solar road modules in the Netherlands. Coefficient c_5 equals zero because in the case of solar roads, no ground reflected irradiance component is considered.

[kWh/m^2/y]	c_1	c_2	c_3	c_4	c_5	Sum
South-West	549	147	−81	441	0	1026
North-East	482	257	−163	406	0	982

Table A2
DC yield coefficients for 0° tilted solar road modules in the Netherlands. Coefficient d_5 equals zero because in the case of solar roads, no ground reflected irradiance component is considered.

[kWh/y] poly c-Si	d_1	d_2	d_3	d_4	d_5	Sum
South-West	86	27	−15	63	0	160
North-East	74	46	−29	62	0	153
[kWh/y] mono c-Si	**d_1**	**d_2**	**d_3**	**d_4**	**d_5**	**Sum**
South-West	108	33	−19	79	0	201
North-East	94	56	−35	79	0	982
[kWh/y] CIGS	**d_1**	**d_2**	**d_3**	**d_4**	**d_5**	**Sum**
South-West	56	18	−10	41	0	105
North-East	48	30	−19	41	0	100

B. National level irradiation and DC yield potential map

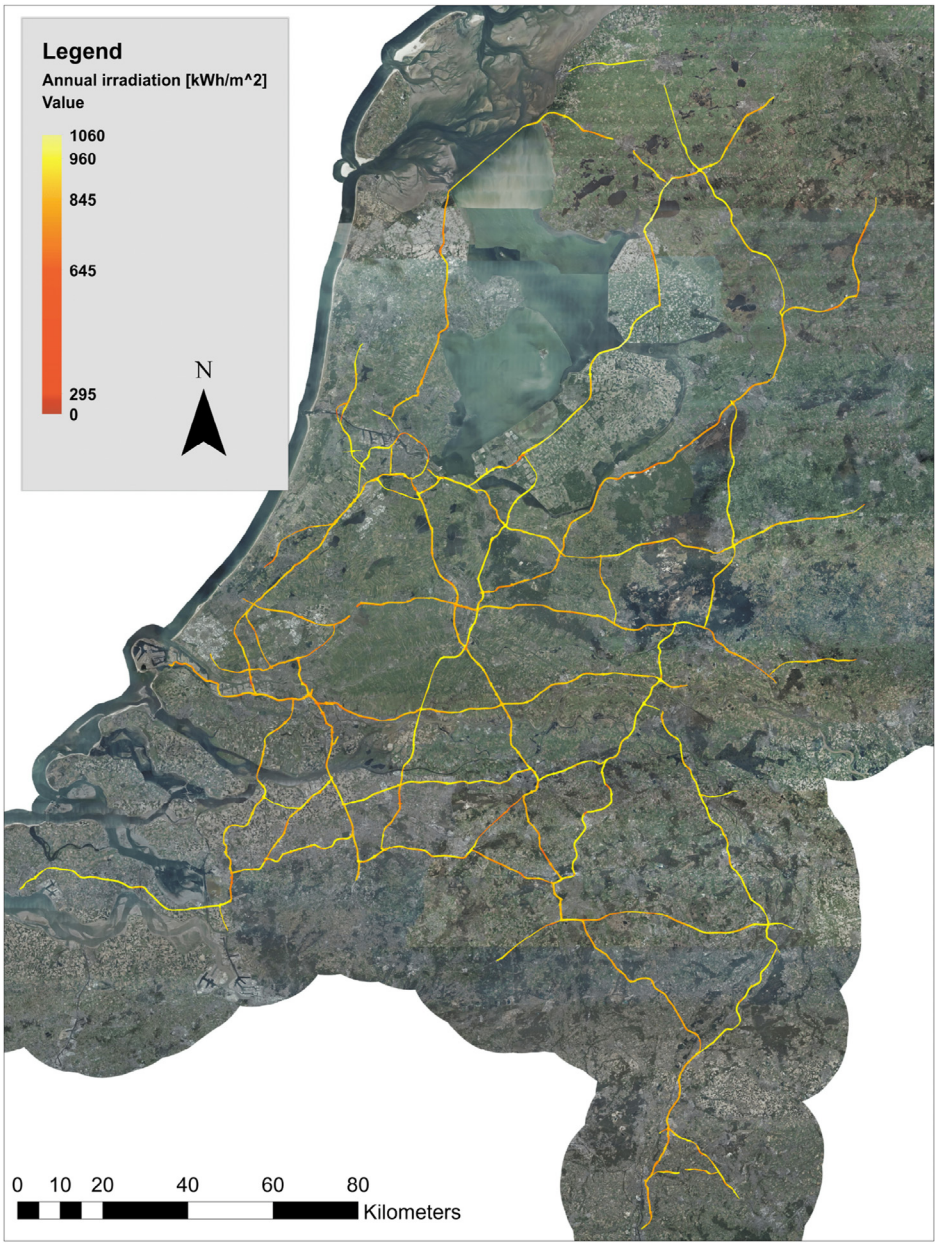

Fig. B1. Potential irradiation map of solar highways in the Netherlands..

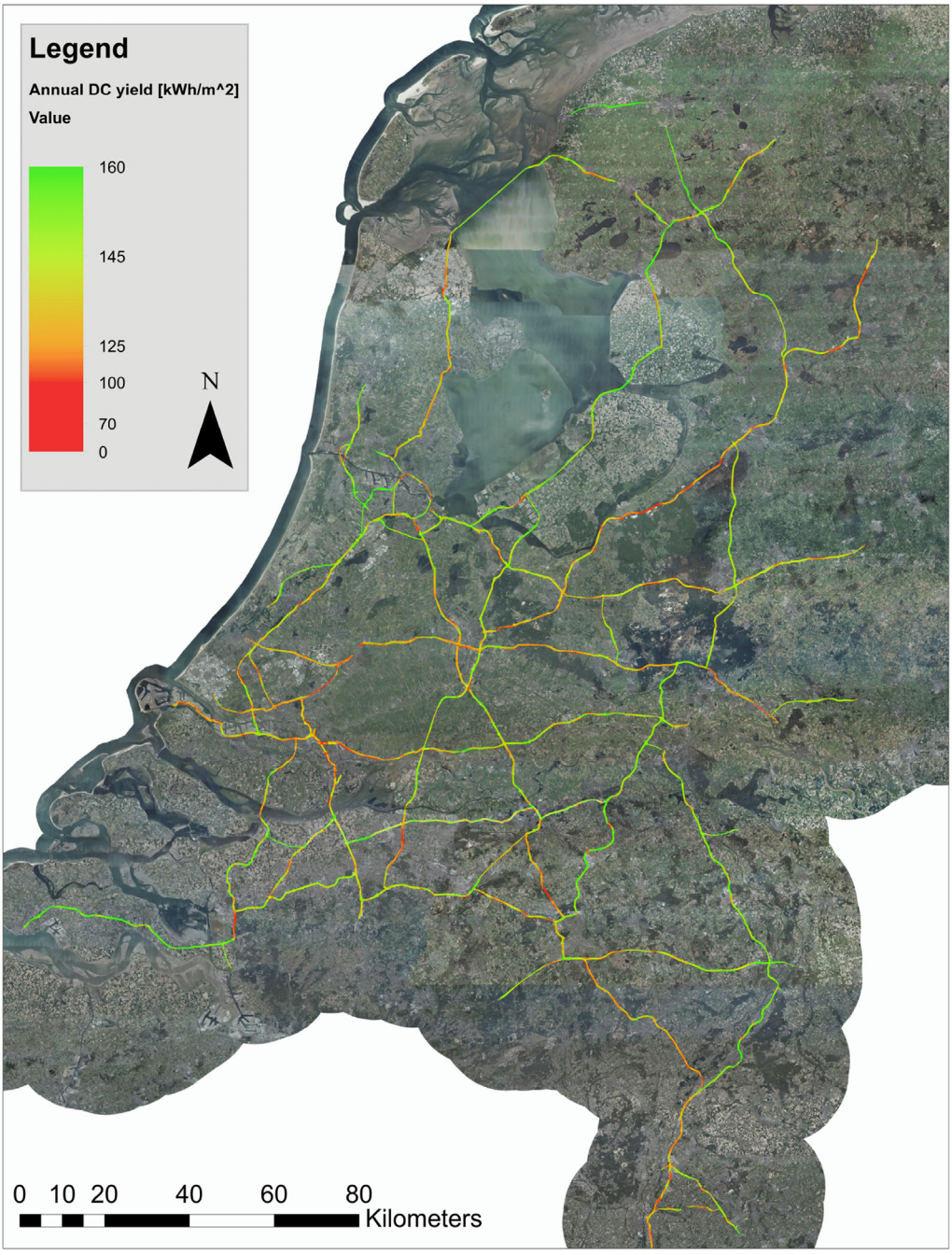

Fig. B2. Potential DC yield map of solar highways in the Netherlands assuming poly c-Si as the to be installed technology. The average output is almost 139 kWh/m^2/y, with peaks of 160 kWh/m^2/y..

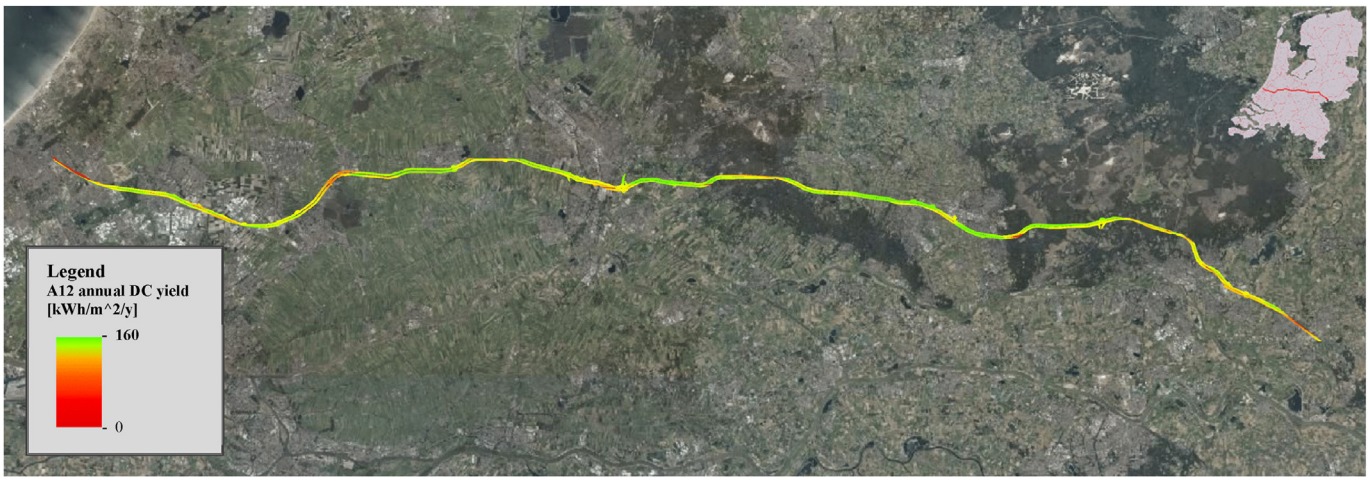

Fig. B3. DC yield potential for poly c-Si of A12 after yield reduction due to traffic shading..

Fig. B4. Traffic coverage time for right and left lane of A12..

References

[1] A. Shekhar, et al., Harvesting roadway solar energy-performance of the installed infrastructure integrated pv bike path, IEEE Journal of Photovoltaics 8 (2018) 1066–1073.

[2] P. Denholm, R.M. Margolis, Land-use requirements and the per-capita solar footprint for photovoltaic generation in the United States, Energy Pol. 36 (2008) 3531–3543.

[3] T. Funabashi, A Gis Approach for Estimating Optimal Sites for Grid-Connected Photovoltaic (Pv) Cells in Nebraska, 2011.

[4] C. Ballif, L. Perret-Aebi, S. Lufkin, E. Rey, Integrated thinking for photovoltaics in buildings, Nature Energy (2018) 438–442.

[5] n-tech Research, BIPV MARKET FORECAST AND ANALYSIS 2018-2027, 2018.

[6] D.E. Attoye, K.A.T. Aoul, A. Hassan, A review on building integrated photovoltaic façade customization potentials, Sustainability 9 (2018) 2287.

[7] A.S. Dezfooli, et al., Solar pavement: a new emerging technology, Sol. Energy 149 (2017) 272–284.

[8] S.d. Wit, Interviewee, *SOLAROAD'S NEW PHASE: A MOTORWAY that ALSO GENERATES ELECTRICITY* [Interview], 7 March 2019.

[9] J.A. Jakubiec, C.F. Reinhart, Towards validated urban photovoltaic potential and solar radiation maps based ON lidar measurements, gis data, and hourly daysim simulations, Proceedings of SimBuild (2012) 628–637.

[10] F. Lindberg, et al., Solar energy on building envelopes-3d modelling in a 2d environment, Sol. Energy 115 (2015) 369–378.

[11] A. Carcabrini, H. Ziar, O. Isabella, M. Zeman, A simplified skyline-based method for estimating the annual solar energy potential in urban environments, Nature Energy 4 (2019) 206–215.

[12] S. Ahmad, M. Abdul Mujeebu, M.A. Farooqi, Energy harvesting from pavements and roadways: a comprehensive review of technologies, materials, and challenges, Int. J. Energy Res. 55 (2) (2019) 414.

[13] Venugopal Prasanth, et al., Green energy based inductive Self-Healing highways of the future, in: IEEE Transportation Electrification Conference and Expo (ITEC), 2016.

[14] V.K. Kumaravel, Energy Yield Modelling and Validation of SolaRoad, Technical University of Delft, Delft, 2016.

[15] TNO, SOLAROAD: THE ROAD THAT GENERATES POWER, 25 February 2016.

[16] TNO, "SolaRoad," 2011.

[17] Wattway," Colas, [Online]. Available: http://www.wattwaybycolas.com/en/.. [Accessed 2019 August 6th].

[18] E. van Gastel, M. de Jonge Baas, BAM Infra stopt proef met zonnewegdek: 'Potentie aanwezig, maar verdere ontwikkeling nodig', Solar Magazine 8 (20 May 2019). https://solarmagazine.nl/nieuws-zonne-energie/i18509/bam-infra-stopt-proef-met-zonnewegdek-potentie-aanwezig-maar-verdere-ontwikkeling-nodig.

[19] B. Holdsworth, Renewable energy roads, Re-focus (2003) 58–60.

[20] R. Pool, Sunshine highways, Eng. Technol. (2011) 54–57.

[21] Publieke Dienstverlening Op de Kaart (PDOK) [Online]. Available, https://www.pdok.nl/. (Accessed 14 December 2019).

[22] Desktop ArcGIS [Online]. Available: http://desktop.arcgis.com/en/arcmap/10.3/manage-data/las-dataset/what-is-lidar-data-.htm, 20 10 2019.

[23] M. Keijzer, et al., A Multi-Surface Reflected Irradiance Model for Pyranometer Corrections and PV Yield Calculations in Complex Urban Geometries, Technical University of Delft, Delft, 2019.

[24] C. Carneiro, E. Morello, G. Desthieux, F. Golay, Urban environment quality indicators: application to solar radiation and morphological analysis on built area, in: In Proc. 3rd WSEAS International Conference on Visualization, Imaging and Simulation, 2010.

[25] C. Rowe, C. Willmott, Solar irradiance on flat-plate collectors in urban environments, Sol. Energy 33 (3–4) (1984) 343–351.

[26] R. Perez, P. Ineichen, R. Seals, J. Michalsky, R. Stewart, Modeling daylight availability and irradiance components from direct and global irradiance, Sol. Energy 44 (1990) 271–289.

[27] A.B. Meindel, M.P. Meindel, Applied Solar Energy. An Introduction, Addison-

Wesley publishing company, Arizona, 1979.
[28] C.A. Gueymard, et al., Direct solar transmittance and irradiance predictions with broadband models. part i: detailed theoretical performance assessment, Sol. Energy 74 (2003) 355–379.
[29] G. Kopp, J.L. Lean, A new, lower value of total solar irradiance: evidence and climate significance, Geophys. Res. Lett. 38 (1) (2011).
[30] M. K. Fuentes, "A Simplified Thermal Model for Flat-Plate Photovoltaic Arrays".
[31] KNMI Data Centre, Radiation - Transformed Daily Global Radiation, KNMI14, Netherlands," 30 11 2015 [Online]. Available, https://data.knmi.nl/datasets/knmi14_globale_straling/3.2?q=radiation. (Accessed 16 December 2019).
[32] Centraal Bureau voor de Statistiek, Energy Consumption Down in 2018, CBS, 2018.
[33] Sustainability Criteria for Sustainable Public Procurement of Public Lighting Version 1.5, Dutch Ministry of Infrastructure and the Environment, 2011.
[34] M. Hulsebosch, P. Willigenburg, J. Woudstra, B. Groenewald, DIRECT CURRENT IN PUBLIC LIGHTING FOR IMPROVEMENT IN LED PERFORMANCE AND COSTS, Cape Town, South Africa, in: 2014 International Conference on the Eleventh Industrial and Commercial Use of Energy, 19-20 Aug. 2014, 2014.
[35] Centraal Bureau voor Statistiek, A13 Busiest National Motorway in the netherlands, CBS, 2017.
[36] N.M. Pearsall, Introduction to Photovoltaic System Performance, in: The Performance of Photovoltaic (PV) Systems, Woodhead Publishing, 2017, pp. 1–19.
[37] W.G.J.H.M. van Sark, Design and components of photovoltaic systems, in: Comprehensive Renewable Energy, 2012, pp. 679–695.